International Journal of Food Science + Technology

International Journal of Food Science and Technology 2023, **58**, 4849–4859

Original article

Understanding starch digestibility of rice: a study in white rice

Kanyarin Saeva,[1] Khongsak Srikaeo[1]* & Peter A Sopade[2]

1 Faculty of Food and Agricultural Technology, Pibulsongkram Rajabhat University, Muang Phitsanulok 65000, Thailand
2 Food Process Engineering Consultants, Abeokuta Cottage, Tia Lane, Forest Lake, Queensland 4078, Australia

(Received 29 April 2023; Accepted in revised form 7 July 2023)

Summary *In vitro* starch digestibility, chemical, pasting, and gelatinisation properties of 10 uncooked pigmented and non-pigmented Thai white rice were studied. Differing in amylose and starch contents, the samples were also significantly ($P \leq 0.05$) different in pasting and gelatinisation properties, maximum digestible starch (40–53 g/100 g dry starch), and rate of starch digestion (0.028–0.054 min^{-1}). The starch digestograms were adequately described ($r^2 > 0.63$; $P \leq 0.001$) by objective logarithm of slope (Sopade Objective Procedure), modified first-order kinetic, and two-term exponential and non-exponential models to be all truly monophasic. The estimated glycaemic index (g/100 g) ranged from 64 and 84, compared to 41–95 for their brown rice forms (*International Journal of Food Science and Technology*, 2022, **57**, 6699), highlighting how bran and hull components influence starch digestion of polished and non-polished rice. This study is foundational to detailedly understand starch digestibility when the rice is further treated.

Keywords Estimated glycaemic index, modelling starch digestograms, monophasic starch digestogram, objective logarithm of slope, sopade objective procedure, starch digestion.

Introduction

The cultivation of rice, a global food commodity, has increased (≈161–165 million hectares) within the past 10 years (2012–2021) from 728 to 787 million MT (FAOSTAT, 2023). Although rice production in Thailand, respectively, dropped by about 6% and 12% in cultivated area and production during the period, but now recovering (2019–2021) from the impacts of the COVID-19 pandemic, rice was the second most produced food commodity in Thailand in 2021, with about 34 million MT (FAOSTAT, 2023). The most prevalent form of rice consumed is white, milled, or polished rice, which is made by polishing brown rice to remove hulls and bran, revealing starchy endosperms with high starch proportions (Verma & Srivastav, 2021). As widely acknowledged, consumption of white rice elevates blood sugar levels, glycaemia, with associated health issues (Kong *et al*., 2011; Kumar *et al*., 2018; Toutounji *et al*., 2019) that are increasing globally. Strategies to reduce glycaemic response usually focus on slowing starch digestion (Sopade, 2017; Wee & Henry, 2020) through, for example, processing and material selections, the success of which requires a solid understanding of starch digestibility. With *in vitro* starch digestion, techniques that can reveal highly valuable scientific trends, devoid of experimental or computational anomalies, are valuable (Qadir & Wani, 2022).

In vitro starch digestibility of rice continues to interest researchers, with studies on different behaviours and parameters that are dependent on varieties, structural properties, non-starch components, processing, and treatments (Tamura *et al*., 2021; Srikaeo, 2022). More studies are, however, needed to maximally benefit consumers by thoroughly understanding rice varietal effects and properly modelling *in vitro* starch digestograms with reproducible, objective, and consistent procedures. Our previous study (Srikaeo *et al*., 2022) modelled starch digestograms of ten Thai brown rice varieties with novel approaches for mono- and multi-phasic starch digestograms. The present study, on their pigmented and non-pigmented white rice counterparts, builds on the novel baseline, with the objective of understanding the starch digestibility of the white rice varieties and exploring changes in their digestion patterns and modes vis-à-vis the brown rice. This will lead to a systematic understanding of digestibility of starch in processed/treated and/or non-processed/untreated rice for global benefits.

Materials and methods

Rice samples and milling process

Ten varieties of paddy rice, pigmented and non-pigmented, were obtained from several Thailand rice

*Correspondent: E-mail: khongsak@live.psru.ac.th

doi:10.1111/ijfs.16599

research centres in Phitsanulok, Pathum Thani, and Chiang Mai. The varieties, fully described in Srikaeo *et al*. (2022), were of (i) waxy to low amylose, coded wrSP and wrLP; (ii) low to medium amylose, coded wrKD, wrRB, wrHN, wrSY, wrP8, and wrR4; and (iii) high amylose, coded wrP2 and wrR6. The amylose (5.0–31.5 g/100 g solids) and moisture (14 ± 0.72 g/100 g) contents were, respectively, measured by the colorimetric (AACC 61–03.01) and vacuum oven (AACC 44–15.02) methods (AACC, 2010). The paddy rice was dehusked and polished using a pilot milling device (NW 1000; Natrawee Technology Co., Ltd., Chachoengsao, Thailand) to produce white rice (Fig. S1) with a well-milled grade (bran removal to the extent that the rice kernel has a beautiful appearance).

Chemical, functional, and *in vitro* starch digestibility

The white rice was ground (80-mesh screen; Hammer Mill, LM 3100; PerkinElmer Inc., MA, USA) and analysed for the following (Srikaeo *et al*., 2022):

a Total starch, using the Megazyme AA/AMG Assay Kit (AACC Method 76–13.01, AACC, 2010).

b Pasting properties, using the Rapid Visco Analyser (Model 4800; PerkinElmer Inc., MA, USA) with Standard Procedure 1 (13-min, about 3.5 g of sample, and 25 mL distilled water), AACC method 76–21 (AACC, 2010). The pasting parameters were obtained with the RVA ThermoCline for Windows®.

c Gelatinisation properties, using differential scanning calorimetry (Model DSC 1; Mettler Toledo DSC), by hydrating (flour:water ratio of 1:2) overnight (≈25 °C), before weighing (25 ± 5 mg) into aluminium DSC pans (100 μL), hermetically sealed, and heating (25–120 °C at 5 °C/min), with an empty reference pan.

d *In vitro starch* digestibility, using the rapid *in vitro* digestibility assay based on glucometry (Sopade & Gidley, 2009), by treating the ground rice (0.5 g) with α-amylase, pepsin, pancreatin, and amyloglucosidase upon the required pH adjustments and neutralisations. Digested starch (per 100 g dry starch) was periodically measured and calculated from glucose concentrations (Accu-Check® Performa® glucometer).

Modelling starch digestograms

Having proven the objective logarithm of slope procedure, the Sopade Objective Procedure (Sopade, 2021), suitable for the brown rice of the same varieties (Srikaeo *et al*., 2022), it was mainly used in modelling the *in vitro* starch digestograms of the white rice to aid comparisons. The duplicated digested starch data (D_{i}) were pooled together to plot logarithm of slope, LOS, (ln $\{[D_{i+1} - D_i]/[t_{i+1} - t_i]\}$) against time ($t_i$) LOS, TLOS, ($[t_{i+1} + t_i]/2$) and described by polynomial equations of orders 1–3. Appropriate first and/or second derivative(s) of the polynomial equations was or were used to obtain practical critical TLOS, $\mathrm{TLOS_{critical}}$, from which the critical digestion times, t_{critical}, were interpolated for slope changes or discontinuities and the phases/segments of the starch digestograms.

Each starch digestion phase/segment from above, with no discarded experimental data, was subsequently modelled (nonlinear regressions; constrained) by the modified first-order kinetic equation, eqn (1), as described earlier (Sopade, 2022a).

$$D_{t_i} = D_{0_i} + D_{(\infty-0)i}(1-\exp[-K_i t]) \text{ or}$$
$$D_{t_i} = D_{0_i} + (D_{\infty i} - D_{0_i})(1-\exp[-K_i t]) \quad (1)$$

where D_{t_i} = digested starch in phase/segment i at time t, D_{0_i} = digested starch in phase/segment i at the phase/segment time $t = 0$, $D_{(\infty\text{-}0)i} = D_{\infty i} - D_{0_i}$, with $D_{\infty i}$ being digested starch in phase/segment i at time $t \to \infty$, and K_i = rate of starch digestion in phase/segment i. For samples with proven monophasic starch digestograms (one phase/segment, $i = 1$), eqn (1) was used to describe the whole digestogram, while samples with biphasic starch digestograms were also initially described by two-term exponential (eqn 2), and non-exponential (eqn 3) models (Sopade, 2022a) to additionally guide the true digestogram class:

$$D_t = D_0 + D_1\,(1-\exp[-K_1\,t]) + D_2\,(1-\exp[-K_2 t]) \quad (2)$$

where D_1 = digested starch function in phase/segment 1, K_1 = rate of digestion in phase/segment 1, D_2 = digested starch function in phase/segment 2, K_2 = rate of digestion in phase/segment 2, and as $t \to \infty$, $D_\infty = (D_0 + D_1 + D_2)$.

$$D_t = D_0 + \frac{t}{K_{\mathrm{p1}} + K_{\mathrm{p2}}t} + \frac{t}{K_{\mathrm{p3}} + K_{\mathrm{p4}}t} \quad (3)$$

where $1/K_{\mathrm{p1}}$ = rate of digestion in phase/segment 1, $1/K_{\mathrm{p3}}$ = rate of digestion in phase/segment 2, and K_{p2} and K_{p4} are digested starch functions in phases/segments 1 and 2 to define the maximum digestible starch, $D_\infty = (D_0 + [1/K_{\mathrm{p2}}] + [1/K_{\mathrm{p4}}])$, as $t \to \infty$.

Statistical analysis

The Microsoft Excel Solver® (GRG nonlinear method) was simply used, with constraints ($D_0 \geq 0$ g/100 g dry starch, $D_\infty \leq 100$ g/100 g dry starch), for eqns (1–3) to describe the starch digestograms. Sum of squares of residuals (SUMSQ), coefficient of determination (r^2), mean relative deviation modulus (MRDM), and plots of residuals were the predictability indices (Srikaeo *et al*., 2022) for the best model or procedure for the digestograms. Heterogeneity tests (95% confidence intervals, the *t*-test, and coefficients of variation [CV]) were conducted on the rates of starch digestion from the multiphasic digestograms to conclude the true starch digestogram classes (Sopade, 2021).

Results and discussion

Chemical and functional properties

Starch content

The white rice samples revealed a similar total starch content, ranging from about 82–86 g/100 g solids (Table 1) and within reported values for white rice (Toutounji *et al*., 2019). The values are nominally higher than those (Srikaeo *et al*., 2022) for the brown rice forms (66–80 g/100 g solids), which is not unexpected, as polishing concentrates endosperm starch.

Pasting properties

The white rice samples revealed heterogeneous pasting parameters (Table 1) that are also different from those (Srikaeo *et al*., 2022) of their brown rice forms. Pasting properties are influenced by starch and non-starch properties (Meadows, 2002), and the waxy white rice samples, wrSP and wrLP, like their brown rice forms, pasted to a high peak viscosity, with a high breakdown viscosity, as they were highly shear-sensitive, yielding a low final viscosity. Samples wrP2 and wrR6, the high-amylose rice, peaked at a low viscosity and were more resistant to shearing or stirring, leading to low breakdown and high final viscosities, as generally found for high-amylose samples. However, as explained for the brown rice forms (Srikaeo *et al*., 2022), and in view of the pasting viscosities of samples wrSY, wrP8, and wrR4 (medium to high amylose) relative to sample wrKD (low-medium amylose), factors other than amylose (*e.g*., non-starch components, complexes of amylose, molecular structures, and organisations, *etc*.) contribute to final pasting behaviours of starchy-containing foods. Moreover, white rice flours can demonstrate higher peak, hold, breakdown, final, and setback viscosities than brown rice flours because, rice polishing removes bran layers and their rich phytonutrients and dietary fibre to influence starch-related properties (Balet *et al*., 2019).

Gelatinisation properties

Table 1 shows similar gelatinisation temperatures for the rice samples, but sample wrSY, a medium to high-amylose sample, was significantly ($P \leq 0.05$) different from others. Previous research has shown a negative correlation between amylose content and starch gelatinisation enthalpy (ΔH), and much higher gelatinisation temperatures are associated with high-amylose starches (>40%). This is most likely due to the presence of much longer amylopectin chains associated with those high-amylose starches, as opposed to fine amylose structures (Li *et al*., 2019). ΔH reflects the thermal energy associated with crystallite melting, depleting inter- and intra-helical hydrogen bonds, and is generally inversely proportional to amylose content (Zhang *et al*., 2017). As a result, waxy rice samples (wrSP and wrLP) showed the highest ΔH, although not significantly ($P > 0.05$) different from the low to medium amylose rice samples (wrKD, wrRB, and wrHN), while the high-amylose white rice sample wrP2 showed the lowest ΔH. The waxy white rice samples also gelatinised over the widest (Tc−To) temperature range (wrSP, 22.9 °C; wrLP, 20.9 °C). In general, a wider range of gelatinisation temperatures indicates a greater crystallinity heterogeneity, with the least stable crystallites melting at a low temperature (To) and the remaining crystallites melting with increasing difficulty at higher temperatures (Tc). The largest (Tc−To) value for waxy rice suggests amylose is essential for the homogeneous formation of amylopectin crystallites (Li & Gong, 2020). The gelatinisation properties of the white rice samples are similar to their brown rice forms earlier reported (Srikaeo *et al*., 2022), indicating minimal effects of the polishing of the varieties on gelatinisation. Rice polishing can, however, affect starch gelatinisation and other properties to influence starch digestion (Lin *et al*., 2019).

In vitro starch digestibility of the white rice

Slope changes or discontinuities

Table 2 summarises the polynomial equations of orders 1–3 for the LOS-TLOS plots of the samples based on the Sopade Objective Procedure (Sopade, 2021). The polynomial equations adequately described ($P \leq 0.05$) the samples, and Fig. S2 shows typical LOS-TLOS plots, indicating true and preliminary digestogram classes to emphasise differences. From the *F*-values (Table 2), the linear equation (order 1) was the best (lowest *F*-value) for samples wrHN, wrR4, wrP2, and wrR6, the quadratic equation (order 2) was the best for samples wrSP, wrLP, wrSY, and wrP8, and the cubic equation (order 3) was the best for samples wrKD and wrRB. Discarding over-parameterisations in the Sopade Objective Procedure (Sopade, 2021), the cubic equation did not solely describe the samples.

Table 2 reports some non-defined (ND) $TLOS_{critical, practical}$, because the stationary and/or inflection point(s) from the first and/or second derivatives of the appropriate polynomial equation did not leave enough data to be applied, were negative, or higher than the highest digestion time of 120 min (Sopade, 2021, 2022b). Hence, the samples exhibited monophasic starch digestograms, except sample wrRB that was possibly

Table 1 Chemical and functional properties of the white rice

Parameters	Rice samples wrSP	wrLP	wrKD	wrRB	wrHN	wrSY	wrP8	wrR4	wrP2	wrR6
Total starch (g/100 g solids)	83.7 ± 1.34ab	84.6 ± 2.49ab	83.4 ± 0.86ab	83.1 ± 0.57ab	84.0 ± 2.30ab	86.1 ± 1.04a	81.8 ± 1.62b	83.7 ± 0.74ab	84.8 ± 1.10ab	85.2 ± 0.61ab
Pasting properties										
Initial viscosity (cP)	203 ± 18.5c	193 ± 13.7c	268 ± 9.0ab	273 ± 13.9ab	198 ± 16.0c	229 ± 15.1bc	302 ± 11.3a	257 ± 35.9ab	183 ± 3.5c	199 ± 11.4c
Pasting temperature (°C)	74.2 ± 0.08e	72.4 ± 0.48f	88.8 ± 0.05b	88.6 ± 0.52b	86.6 ± 0.88c	90.4 ± 0.01a	84.0 ± 0.05d	83.2 ± 0.75d	90.4 ± 0.80a	88.7 ± 0.08b
Peak viscosity (cP)	3825 ± 59.7a	3605 ± 62.0b	3306 ± 91.2c	3152 ± 28.1d	2453 ± 19.5f	2724 ± 6.51e	3375 ± 41.1c	3697 ± 88.5ab	1277 ± 35.2 g	1313 ± 18.6 g
Trough viscosity (cP)	1279 ± 21.6f	2453 ± 33.7a	2206 ± 53.6c	2153 ± 10.6c	2472 ± 7.4a	2039 ± 2.0d	1941 ± 9.0e	1971 ± 17.0de	1208 ± 25.1f	2372 ± 21.5b
Final viscosity (cP)	2162 ± 7.2 g	3058 ± 25.2f	3864 ± 40.6b	3673 ± 10.6c	3811 ± 15.0b	3390 ± 25.0de	3471 ± 33.5d	3478 ± 27.5d	3338 ± 82.0e	4211 ± 21.5a
Setback viscosity (cP)	883 ± 28.7f	605 ± 10.7 g	1658 ± 38.7c	1520 ± 6.9d	1339 ± 8.7e	1351 ± 27.0e	1530 ± 42.5d	1507 ± 44.5d	2129 ± 57.5a	1838 ± 0.3b
Gelatinisation properties										
Onset temperature (To, °C)	66.2 ± 1.56b	64.7 ± 1.36b	66.0 ± 0.35b	67.4 ± 0.15b	68.2 ± 1.2b	78.1 ± 2.72a	67.9 ± 0.99b	67.0 ± 0.20b	67.5 ± 0.19b	65.8 ± 1.77b
Peak temperature (Tp, °C)	73.5 ± 0.20b	71.2 ± 1.20b	71.6 ± 0.44b	72.3 ± 0.82b	74.7 ± 1.65b	84.3 ± 0.01a	71.9 ± 0.40b	72.4 ± 0.16b	71.9 ± 0.92b	71.86 ± 0.47b
End temperature (Tc, °C)	87.1 ± 5.81ab	87.6 ± 0.24ab	85.1 ± 2.68ab	83.4 ± 6.00ab	87.3 ± 6.65ab	95.2 ± 2.88a	79.4 ± 0.80ab	82.1 ± 5.97ab	79.1 ± 3.17ab	78.1 ± 1.80b
Enthalpy (ΔH, J g^{-1} DS)	4.1 ± 0.63a	3.9 ± 0.08ab	3.2 ± 0.79abc	2.1 ± 0.69abc	2.6 ± 0.22abc	1.8 ± 0.94bc	1.4 ± 0.66c	1.4 ± 0.08c	1.3 ± 0.30c	1.6 ± 0.08c
Temperature range (Tc–To, °C)	20.9	22.9	19.1	16.0	19.1	17.1	11.5	15.1	11.6	12.3

Values are means ± standard deviations (duplicate). Means that do not share a letter in a row are significantly different ($P \leq 0.05$). DS = Dry starch.

Table 2 Polynomial equations for the objective logarithm of slope (the Sopade Objective Procedure)

	The Sopade Objective Procedure		
Rice samples/Regression parameters	**Linear, First-order polynomial**	**Quadratic, Second-order polynomial**	**Cubic, Third-order polynomial**
wrSP	$\text{LOS} = (-2.6 \times 10^{-2})\ \text{TLOS} + 0.38$	$\text{LOS} = (3.6 \times 10^{-4})\ \text{TLOS}^2 - (6.3 \times 10^{-2})\ \text{TLOS} + 0.89$	$\text{LOS} = (-1.0 \times 10^{-7})\ \text{TLOS}^3 + (3.7 \times 10^{-4})\ \text{TLOS}^2 - (6.3 \times 10^{-2})\ \text{TLOS} + 0.89$
r^2	0.831	0.966	0.966
F-value	1.40×10^{-7}	**9.27×10^{-12}**	1.56×10^{-10}
TLOS critical, practical (min.)	NA	ND	ND
Inference (final)	Monophasic		
wrLP	$\text{LOS} = (-2.6 \times 10^{-2})\ \text{TLOS} + 0.31$	$\text{LOS} = (6.1 \times 10^{-4})\ \text{TLOS}^2 - (8.9 \times 10^{-2})\ \text{TLOS} + 1.17$	$\text{LOS} = (4.9 \times 10^{-6})\ \text{TLOS}^3 - (1.8 \times 10^{-4})\ \text{TLOS}^2 - (5.8 \times 10^{-2})\ \text{TLOS} + 0.94$
r^2	0.631	0.924	0.937
F-value	8.22×10^{-5}	**4.13×10^{-9}**	1.25×10^{-8}
TLOS critical, practical (min.)	NA	ND	ND
Inference (final)	Monophasic		
wrKD	$\text{LOS} = (-2.9 \times 10^{-2})\ \text{TLOS} + 0.38$	$\text{LOS} = (2.4 \times 10^{-4})\ \text{TLOS}^2 - (5.5 \times 10^{-2})\ \text{TLOS} + 0.72$	$\text{LOS} = (-1.1 \times 10^{-5})\ \text{TLOS}^3 + (2.0 \times 10^{-3})\ \text{TLOS}^2 - (1.2 \times 10^{-1})\ \text{TLOS} + 1.23$
r^2	0.816	0.862	0.924
F-value	2.84×10^{-7}	3.50×10^{-7}	**4.31×10^{-8}**
TLOS critical, practical (min.)	NA	ND	ND
Inference (final)	Monophasic		
wrRB	$\text{LOS} = (-4.1 \times 10^{-2})\ \text{TLOS} + 0.51$	$\text{LOS} = (4.4 \times 10^{-4})\ \text{TLOS}^2 - (8.6 \times 10^{-2})\ \text{TLOS} + 1.14$	$\text{LOS} = (1.1 \times 10^{-5})\ \text{TLOS}^3 - (1.3 \times 10^{-3})\ \text{TLOS}^2 - (1.6 \times 10^{-2})\ \text{TLOS} + 0.60$
r^2	0.817	0.898	0.933
F-value	2.68×10^{-7}	3.70×10^{-8}	**1.91×10^{-8}**
TLOS critical, practical (min.)	NA	ND	45.3
Inference (preliminary)	Biphasic		
wrHN	$\text{LOS} = (-3.4 \times 10^{-2})\ \text{TLOS} + 0.47$	$\text{LOS} = (-4.8 \times 10^{-5})\ \text{TLOS}^2 - (2.9 \times 10^{-2})\ \text{TLOS} + 0.40$	$\text{LOS} = (-1.3 \times 10^{-5})\ \text{TLOS}^3 + (2.0 \times 10^{-3})\ \text{TLOS}^2 - (1.1 \times 10^{-1})\ \text{TLOS} + 1.02$
r^2	0.815	0.817	0.885
F-value	**2.91×10^{-7}**	2.98×10^{-6}	8.17×10^{-7}
TLOS critical, practical (min.)	NA	ND	ND
Inference (final)	Monophasic		
wrSY	$\text{LOS} = (-2.4 \times 10^{-2})\ \text{TLOS} - 0.02$	$\text{LOS} = (3.1 \times 10^{-4})\ \text{TLOS}^2 - (5.6 \times 10^{-2})\ \text{TLOS} + 0.56$	$\text{LOS} = (-6.9 \times 10^{-6})\ \text{TLOS}^3 + (1.4 \times 10^{-3})\ \text{TLOS}^2 - (1.0 \times 10^{-1})\ \text{TLOS} + 0.89$
r^2	0.702	0.797	0.829
F-value	1.43×10^{-5}	**6.35×10^{-6}**	1.21×10^{-5}
TLOS critical, practical (min.)	NA	ND	ND
Inference (final)	Monophasic		
wrP8	$\text{LOS} = (-2.4 \times 10^{-2})\ \text{TLOS} + 0.15$	$\text{LOS} = (3.4 \times 10^{-4})\ \text{TLOS}^2 - (5.9 \times 10^{-2})\ \text{TLOS} + 0.63$	$\text{LOS} = (4.8 \times 10^{-6})\ \text{TLOS}^3 - (4.3 \times 10^{-4})\ \text{TLOS}^2 - (2.8 \times 10^{-2})\ \text{TLOS} + 0.40$
r^2	0.706	0.829	0.845
F-value	1.28×10^{-5}	**1.78×10^{-6}**	6.20×10^{-6}
TLOS critical, practical (min.)	NA	ND	ND
Inference (final)	Monophasic		
wrR4	$\text{LOS} = (-3.7 \times 10^{-2})\ \text{TLOS} + 0.30$	$\text{LOS} = (2.9 \times 10^{-4})\ \text{TLOS}^2 - (6.7 \times 10^{-2})\ \text{TLOS} + 0.71$	$\text{LOS} = (4.5 \times 10^{-6})\ \text{TLOS}^3 - (4.3 \times 10^{-4})\ \text{TLOS}^2 - (3.9 \times 10^{-2})\ \text{TLOS} + 0.50$
r^2	0.746	0.783	0.790
F-value	**3.84×10^{-6}**	1.40×10^{-5}	5.19×10^{-5}

Table 2 (*Continued*)

Rice samples/Regression parameters	The Sopade Objective Procedure Linear, First-order polynomial	Quadratic, Second-order polynomial	Cubic, Third-order polynomial
TLOS critical, practical (min.)	NA	ND	ND
Inference (final)	Monophasic		
wrP2	LOS = (-3.0×10^{-2}) TLOS + 0.20	LOS = (1.0×10^{-4}) TLOS^2 − (4.1×10^{-2}) TLOS + 0.35	LOS = (-1.2×10^{-6}) TLOS^3 + (2.9×10^{-4}) TLOS^2 − (4.8×10^{-2}) TLOS + 0.41
r^2	0.958	0.968	0.969
F-value	**1.76×10^{-12}**	6.58×10^{-12}	9.42×10^{-11}
TLOS critical, practical (min.)	NA	ND	ND
Inference (final)	Monophasic		
wrR6	LOS = (-5.5×10^{-2}) TLOS + 0.79	LOS = (1.2×10^{-5}) TLOS^2 − (5.6×10^{-2}) TLOS + 0.80	LOS = (4.9×10^{-6}) TLOS^3 − (7.7×10^{-4}) TLOS^2 − (2.5×10^{-2}) TLOS + 0.57
r^2	0.971	0.971	0.975
F-value	**1.13×10^{-13}**	3.27×10^{-12}	1.92×10^{-11}
TLOS critical, practical (min.)	NA	ND	ND
Inference (final)	Monophasic		

LOS, Logarithm of slope (= ln $[D_{t_{n+1}} - D_{t_n}]/\{t_n + 1 - t_n\}$); TLOS = Logarithm of slope time (= $[t_{n+1} + t_n]/2$); NA, Not applicable; ND, Not defined or Non-practical. Bold *F*-values are the lowest.

biphasic in starch digestion, but no samples indicated triphasic starch digestograms (Table 2). Deeply probing the preliminary biphasic phenomenon in sample wrRB, Table S1 shows the heterogeneity test (95% confidence interval, *t*-test, and CV) on the predicted rates of starch digestion from the Sopade Objective Procedure and the two-term models. The Procedure was the best of the three, in terms of the predictability indices, and while the two-term non-exponential model suggested a true biphasic digestograms, both the Procedure and two-term exponential model confirmed (overlapped 95% confidence intervals and non-significant *t*-test) sample wrRB to be truly monophasic. We are, however, aware of the high SD of one of the rates of the preliminary biphasic digestograms, but the Dixon *Q*-test (Rorabacher, 1991; Forestier & Sopade, 2022) for outliers only applies to ≥3 sample sizes. This heterogeneity test again shows the benefits of analysing starch digestograms with a few models to choose the best. Our previous study (Srikaeo *et al.*, 2022) on the brown forms already recommended the Sopade Objective Procedure as the best modelling approach for these rice varieties, which is strengthened in the present study and with sample wrRB.

Hence, all the white rice samples solely and objectively exhibited monophasic starch digestograms, and Fig. 1 typifies the predicted starch digestograms, indicating the suitability of the Procedure ($r^2 \geq 0.975$, $P \leq 0.05$; SUMSQ ≤ 3.2; MRDM ≤ 2.6; Table S2), in describing the *in vitro* starch digestibility of the white rice. Our previous study (Srikaeo *et al.*, 2022) revealed biphasic (rapid-slow and slow-rapid) digestograms in the brown rice forms of rbKD, rbR4, rbRB, and rbSY, which polishing changed to monophasic digestograms in the white rice (wrKD, wrR4, wrRB, and wrSY). Therefore, the polishing, removal of the hulls and brans, and most of, if not, all their non-starch components, possibly removed initial or final hindrances to starch digestion in the white rice that would have, respectively, led to rapid–slow or slow-rapid biphasic digestograms, measured in the brown rice forms. Rice milling or polishing removes bran layers from brown rice (Fig. S1) to influence rice nutritional profiles (Paiva *et al.*, 2014), and the present study established patterns and modes of starch digestion were affected by rice milling or polishing, which has not been solidly and objectively established before. It is worth noting that both the pigmented and non-pigmented white rice exhibited monophasic starch digestograms possibly because the polishing or milling substantially removed the pigments with the bran layers (Fig. S1), as demonstrated by Paiva *et al.* (2014). The pigmented brown rice forms (rbLP, rbHN, rbRB, and rbSY; Srikaeo *et al.*, 2022), however, revealed mono- and bi-phasic starch digestograms, with the biphasic rbRB (rapid-slow) and rbSY (slow-rapid) even showing opposite starch digestion phenomena. As with food systems, rice pigments are made up of many compounds and dependent on degree of rice polishing or milling (Paiva *et al.*, 2014, 2016) to differently modulate starch digestibility.

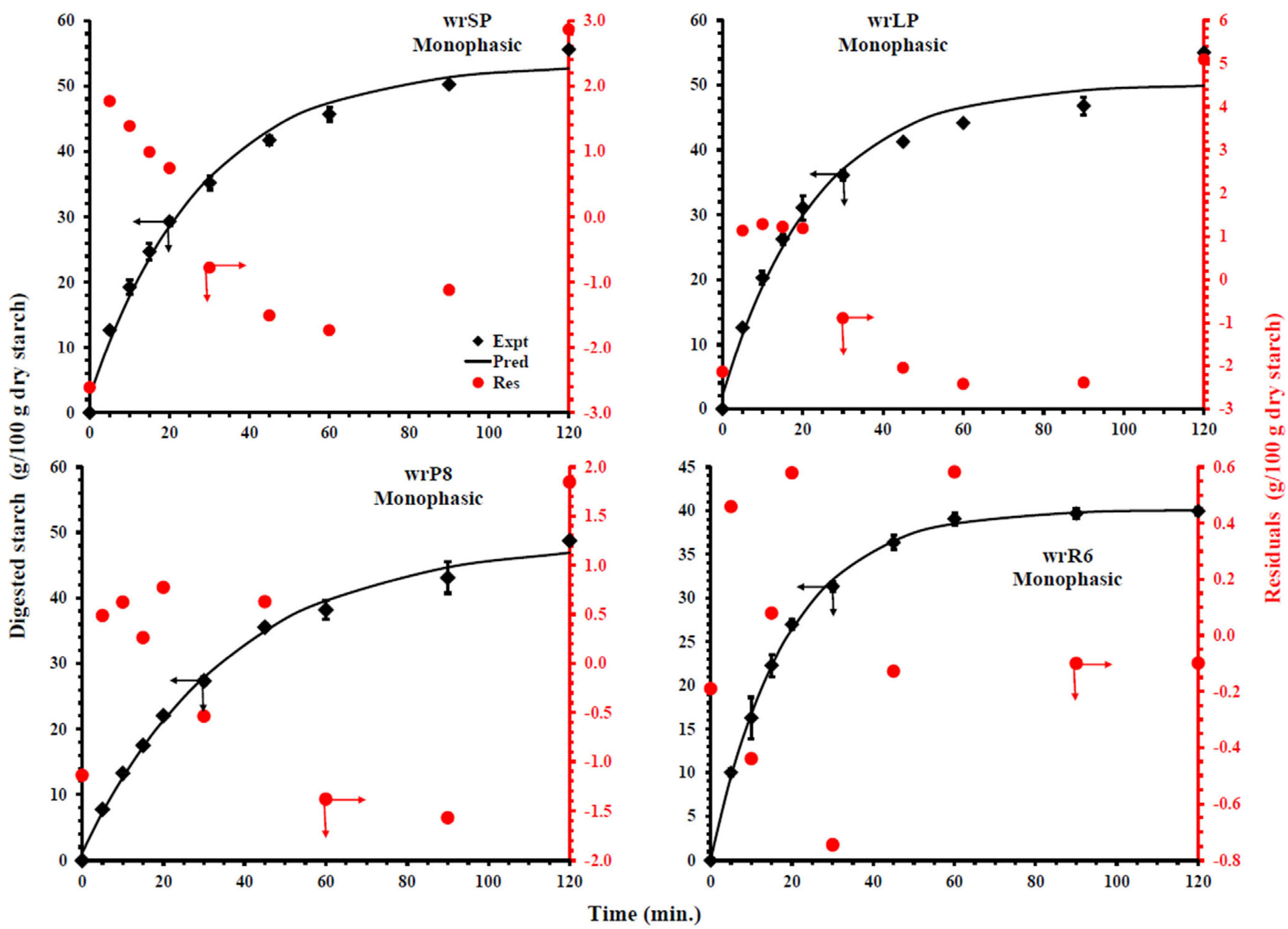

Figure 1 Experimental (Expt) and predicted (Pred) digestograms showing the residuals (Res) of the predictions for typical samples (Error bars are standard deviations).

Starch digestion parameters and estimated glycaemic index
Using the Sopade Objective Procedure, the *in vitro* starch digestion parameters of the samples are summarised in Fig. 2a–d (Table S2). In addition, the comparison of digestion parameters of the monophasic raw brown (Srikaeo *et al*., 2022) and white rice in this study is shown in Table S3. Estimated glycaemic indices, eGIs, of foods are valuable, and for uncooked foods, rice in the present study, eGIs provide a baseline to build an understanding of further processing, treatments, and preparations. Rice, for example, are cooked or prepared in different ways, and understanding non-processed, non-treated, or uncooked rice establishes the necessary baseline, with no compounding effects of cooking, to comprehend the effects of further treatments and handlings of the varieties in the present study.

The eGI values of the white rice samples were obtained by calculating the areas under the digestograms from 0 to 120 min (Srikaeo *et al*., 2011, 2022; Sopade, 2022a, 2022b) relative to that of the white wheat bread described in Petchoo *et al*. (2021) to define the hydrolysis indices (HI = sample digestogram area/bread digestogram area) of the samples. With the white rice all truly exhibiting monophasic starch digestograms, the area under each digestogram from 0 to 120 min was calculated using eqn (4), and the average eGI values (eGI_{AVG}) were calculated using eqn (5), as detailed elsewhere (Sopade, 2017, 2022a).

$$\int_{t_1\,(=0)}^{t_2\,(=120)} D_0 + D_{\infty-0}\left(1-\exp\left[-Kt\right]\right) = \left[D_0 t + D_{\infty-0} t + \frac{D_{\infty-0}}{K}\exp(-Kt)\right]_0^{120} \text{ or } \left[D_{\infty} t + \frac{D_{\infty-0}}{K}\exp(-Kt)\right]_0^{120} \quad (4)$$

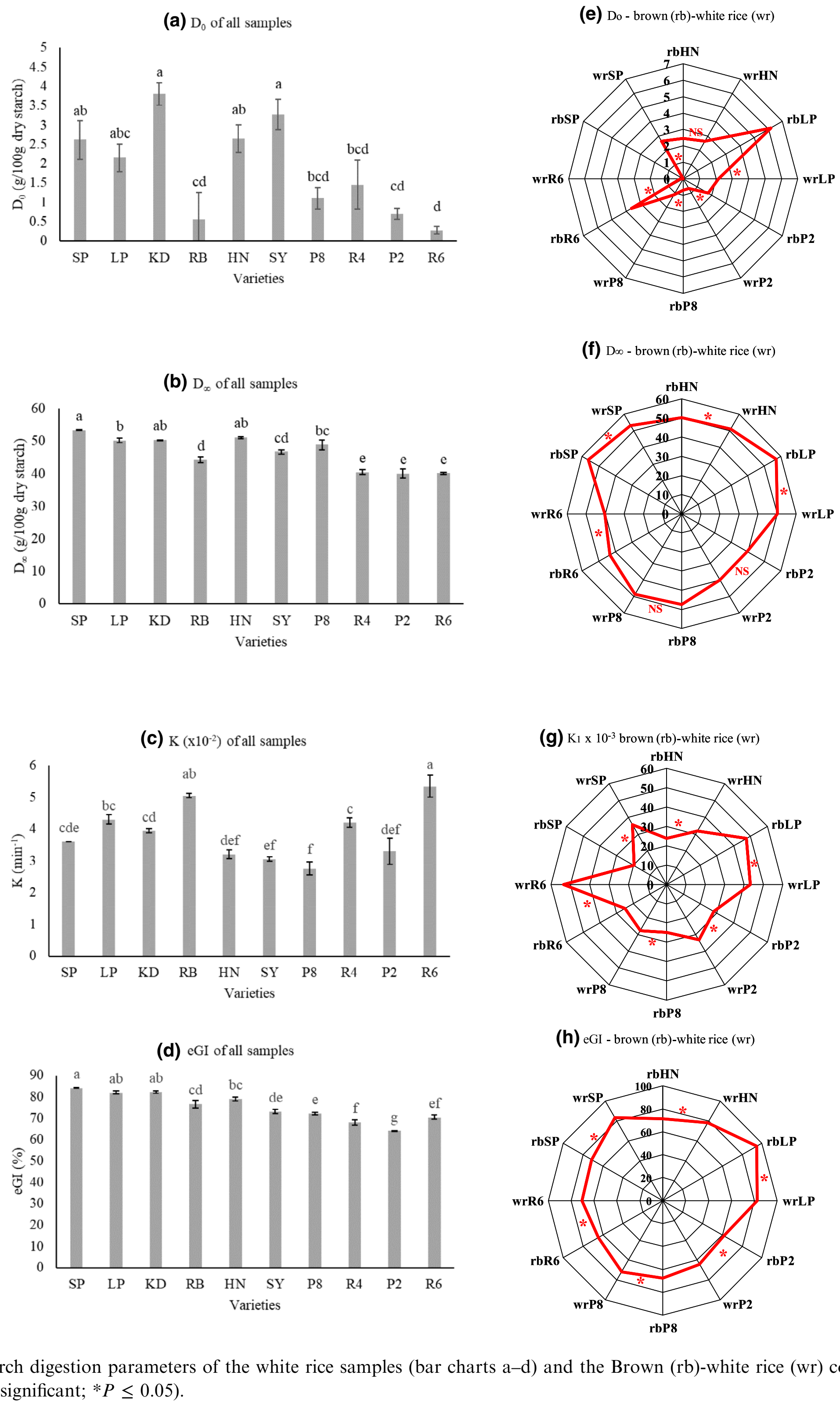

Figure 2 *In vitro* starch digestion parameters of the white rice samples (bar charts a–d) and the Brown (rb)-white rice (wr) comparisons (radar charts e–h; NS, non-significant; $*P \leq 0.05$).

$$eGI_{AVG} = \frac{(26.10 + 0.69HI) + 1.01HI}{2}. \quad (5)$$

The eGIs of the white rice ranged from 64 to 84 g/100 g (Fig. 2d and Table S2), with samples wrSP and wrLP, the waxy varieties, revealing the highest eGI, while the lowest eGI was obtained from wrP2 with the highest amylose content. Although the eGI–amylose content relationship of the white rice samples revealed an inverse trend, it is worth stating that amylose is not the only factor determining starch digestibility especially in intermediate and high-amylose rice (Hu *et al*., 2004). Amylose fine molecular structures play a role in rice digestibility (Gong *et al*., 2019), while native rice starches with shorter amylopectin short chains (DP 10–26) have been revealed to have more perfectly aligned crystalline lamellae and much slower digestion rates than other starches (Li *et al*., 2021). Possibly non-starch micro- and macro-components also play a role, as our study (Srikaeo *et al*., 2022) on the brown rice forms showed the starch digestibility parameters were independent of the amylose contents. The other digestion parameters, very rapidly (salivary–gastric) digestible starch, D_0 (0.2–3.8 g/100 g dry starch; Fig. 2a), maximum digestible starch, D_∞ (39.9–53.4 g/100 g dry starch; Fig. 2b), and rate of starch digestion, K_1 (0.028–0.054 min^{-1}, Fig. 2c) were differently ($P \le 0.05$) defined by the white rice varieties. It is noteworthy that the digestion parameters in the present study are different from those in Srikaeo *et al*. (2022), even from the same varieties. The samples in the present study were obtained from research institutes, while those in Srikaeo *et al*. (2022) were obtained from local markets. Market samples, possibly mixtures from different farms/suppliers, are not expected to be as genetically pure as samples from research institutes. There could also be agronomical/environmental differences that are known to influence food properties.

The effects of the polishing on the rice varieties were further probed by examining the digestion parameters of varieties SP, LP, HN, P8, P2, and R6 that were monophasic in both brown (Srikaeo *et al*., 2022) and white (this study) forms. While polishing was not a variable in this study, as the varieties were polished to only the market eating level, the stated varieties provide insights into the different effects of polishing that might be varietal dependent. Apart from variety LP, a waxy pigmented rice, showing its brown form was more digestible than its white form, the white rice samples had significantly ($P \le 0.05$) higher rate of starch digestion, K_1 (Fig. 2g) and eGI (Fig. 2h) than the brown forms. However, there are no clear effects of the polishing on the very rapid, salivary–gastric, D_0 (Fig. 2e) and maximum, D_∞ (Fig. 2f) digestible starches. Hence, while bran and hull removals affect rice starch digestibility, this depends on other factors/interactions, which need be objectively established. It is noteworthy also that despite the higher concentration of rice bran pigments in the brown form of sample LP (rbLP) than the white form (wrLP), wrLP was less digestible. However, the higher concentration of rice bran pigments in the pigmented brown rice HN (rbHN), among other components, possibly slowed its digestibility relative to the white rice form (wrHN). Although the present study did mandate bran pigment-starch digestibility relationships in rice, the observations with the rice varieties demand studies on such relationships using a robust *in vitro* starch digestion technique with a novel starch digestogram modelling approach, as presented. This will demand knowing the characteristics of the pigments in a progressive study for their inhibitory and/or contributory effects on rice starch digestibility. Having established the trends with the raw brown and white rice, the effects of cooking, for example, on the varieties can be better understood, as systematically explored in further studies.

Conclusions

In vitro starch digestion of ten raw Thai white rice revealed monophasic starch digestograms in the samples, as analysed by objective logarithm of slope, the Sopade Objective Procedure. Multiterm exponential and non-exponential models, backed up with heterogeneity tests, were used to support the Procedure in confirming the true digestogram class of the samples. The samples showed differences in their digestion parameters, as well as their starch and amylose contents, and pasting and gelatinisation properties. While all the white rice samples exhibited monophasic starch digestograms, their brown rice forms revealed both mono- and bi-phasic digestograms. Moreover, for the brown rice forms that revealed monophasic digestograms, their digestion parameters were different from the white rice samples, highlighting the rice polishing modified the patterns and modes of starch digestion. This will help understanding the starch digestibility of the samples when further processed/treated, as in different cooking techniques for consumption.

Acknowledgments

This research was supported by Pibulsongkram Rajabhat University (grant number RDI-1-64-4).

Author contributions

Kanyarin Saeva: Data curation (equal); formal analysis (equal); investigation (equal); methodology (equal).

Khongsak Srikaeo: Conceptualization (equal); data curation (equal); formal analysis (equal); funding acquisition (equal); investigation (equal); methodology (equal); project administration (equal). **Peter Adeoye Sopade:** Conceptualization (equal); data curation (equal); formal analysis (equal); investigation (equal); methodology (equal); project administration (equal).

Conflict of interest statement

The authors declare no conflicting interests.

Ethical approval

Ethics approval was not required for this research.

Peer review

The peer review history for this article is available at https://www.webofscience.com/api/gateway/wos/peer-review/10.1111/ijfs.16599.

Data availability statement

The data that support the findings of this study are available on request from the corresponding author.

References

AACC (2010). *American Association of Cereal Chemists Approved Methods of Analysis*, 11th edn. Minnesota, USA: Cereals and Grains Association.

Balet, S., Guelpa, A., Fox, G. & Manley, M. (2019). Rapid Visco Analyser (RVA) as a tool for measuring starch-related physiochemical properties in cereals: a review. *Food Analytical Methods*, **12**, 2344–2360.

FAOSTAT. (2023). Production – Crops and Livestock Products. Available from: https://www.fao.org/faostat/en/#data/QCL [Accessed 1st April 2023].

Forestier, M. & Sopade, P.A. (2022). Kinetics of starch digestion in potato (*Solanum tuberosum*) flours: innovative modelling and relationships with particle size. *Journal of Food Engineering*, **329**, 111089.

Gong, B., Cheng, L., Gilbert, R.G. & Li, C. (2019). Distribution of short to medium amylose chains are major controllers of *in vitro* digestion of retrograded rice starch. *Food Hydrocolloids*, **96**, 634–643.

Hu, P., Zhao, H., Duan, Z., Linlin, Z. & Wu, D. (2004). Starch digestibility and the estimated glycemic score of different types of rice differing in amylose contents. *Journal of Cereal Science*, **40**, 231–237.

Kong, F., Oztop, M.H., Singh, R.P. & McCarthy, M.J. (2011). Physical changes in white and brown rice during simulated gastric digestion. *Journal of Food Science*, **76**, E450–E457.

Kumar, A., Sahoo, U., Baisakha, B. *et al.* (2018). Resistant starch could be decisive in determining the glycemic index of rice cultivars. *Journal of Cereal Science*, **79**, 348–353.

Li, C. & Gong, B. (2020). Insights into chain-length distributions of amylopectin and amylose molecules on the gelatinization property of rice starches. *International Journal of Biological Macromolecules*, **155**, 721–729.

Li, C., Hu, Y., Gu, F. & Gong, B. (2021). Causal relations among starch fine molecular structure, lamellar/crystalline structure and *in vitro* digestion kinetics of native rice starch. *Food & Function*, **12**, 682–695.

Li, H., Dhital, S., Slade, A.J., Yu, W., Gilbert, R.G. & Gidley, M.J. (2019). Altering starch branching enzymes in wheat generates high-amylose starch with novel molecular structure and functional properties. *Food Hydrocolloids*, **92**, 51–59.

Lin, L., Pan, T., Liu, Q. & Wei, C. (2019). Cooking, morphological, mechanical and digestion properties of cooked rice with suppression of starch branching enzymes. *International Journal of Biological Macromolecules*, **137**, 187–196.

Meadows, F. (2002). Pasting process in rice flour using rapid visco analyser curves and first derivatives. *Cereal Chemistry*, **79**, 559–562.

Pasting properties of rice.

Paiva, F.F., Vanier, N.L., Berrios, J.J. *et al.* (2014). Physicochemical and nutritional properties of pigmented rice subjected to different degrees of milling. *Journal of Food Composition and Analysis*, **35**, 10–17.

Paiva, F.F., Vanier, N.L., Berrios, J.J. *et al.* (2016). Polishing and parboiling effect on the nutrient and technological properties of pigmented rice. *Food Chemistry*, **191**, 105–112.

Petchoo, J., Jittinandana, S., Tuntipopipat, S., Ngampeerapong, C. & Tangsuphoom, N. (2021). Effect of partial substitution of wheat flour with resistant starch on physicochemical, sensorial and nutritional properties of breadsticks. *International Journal of Food Science and Technology*, **56**, 1750–1758.

Qadir, N. & Wani, I.A. (2022). *In-vitro* digestibility of rice starch and factors regulating its digestion process: a review. *Carbohydrate Polymers*, **291**, 119600.

In vitro starch digestibility of rice.

Rorabacher, D.R. (1991). Statistical treatment for rejection of deviant values: critical values of Dixon's "Q" parameter and related subrange ratios at the 95% confidence level. *Analytical Chemistry*, **63**, 139–146.

Dixon-Q test for outliers.

Sopade, P.A. (2017). Cereal processing and glycaemic response. *International Journal of Food Science and Technology*, **52**, 22–37.

Sopade, P.A. (2021). Modelling multiphasic starch digestograms: an objective procedure for slope discontinuities. *International Journal of Food Science & Technology*, **56**, 2651–2661.

Objective logarithm of slope.

Sopade, P.A. (2022a). Modelling multiphasic starch digestograms with multiterm exponential and non-exponential equations. *Carbohydrate Polymers*, **275**, 118698.

Sopade, P.A. (2022b). Homogeneities in *in vitro* starch digestion of compositionally heterogenous white wheat breads. *International Journal of Food Science & Technology*, **57**, 4380–4391.

Sopade, P.A. & Gidley, M.J. (2009). A rapid *in-vitro* digestibility assay based on glucometry for investigating kinetics of starch digestion. *Starch/Staerke*, **61**, 245–255.

Srikaeo, K. (2022). Application of a rapid *in vitro* method based on glucometer for determination of starch digestibility and estimated glycemic index in rice. *Starch*, **75**, 2200174.

Srikaeo, K., Mingyai, S. & Sopade, P.A. (2011). Physicochemical properties, resistant starch content and enzymatic digestibility of unripe banana, edible canna, taro flours and their rice noodle products. *International Journal of Food Science & Technology*, **46**, 2111–2117.

Srikaeo, K., Saeva, K. & Sopade, P.A. (2022). Understanding starch digestibility of rice: a study in brown rice. *International Journal of Food Science & Technology*, **57**, 6699–6710.

Tamura, M., Kumagai, C., Kaur, L., Ogawa, Y. & Singh, J. (2021). Cooking of short, medium and long-grain rice in limited and excess water: effects on microstructural characteristics and gastro-small intestinal starch digestion *in vitro*. *LWT*, **146**, 111379.

Toutounji, M.R., Farahnaky, A., Santhakumar, A.B., Oli, P., Butardo, V.M. & Blanchard, C.L. (2019). Intrinsic and extrinsic

factors affecting rice starch digestibility. *Trends in Food Science & Technology*, **88**, 10–22.
Verma, D.K. & Srivastav, P.P. (2021). Isolation, modification, and characterization of rice starch with emphasis on functional properties and industrial application: a review. *Critical Reviews in Food Science and Nutrition*, **62**, 6577–6604.
Wee, M.S.M. & Henry, C.J. (2020). Reducing the glycemic impact of carbohydrates on foods and meals: strategies for the food industry and consumers with special focus on Asia. *Comprehensive Reviews in Food Science and Food Safety*, **19**, 670–702.
Zhang, C., Chen, S., Ren, X. *et al.* (2017). Molecular structure and physicochemical properties of starches from rice with different amylose contents resulting from modification of OsGBSSI activity. *Journal of Agricultural and Food Chemistry*, **65**, 2222–2232.

Supporting Information

Additional Supporting Information may be found in the online version of this article:

Figure S1. The photos of the samples as brown and white rice: *San-pah-tawng* (SP), *Leum Pua* (LP), *Khao Dawk Mali 105* (KD), *Riceberry* (RB), *Hom Nil* (HN), *Sang Yod Phattalung* (SY), *Phitsanulok 80* (P8), *RD 43* (R4), *Phitsanulok 2* (P2) *and RD 61* (R6).

Figure S2. Typical logarithm of slope (LOS) plots showing one (monophasic) or two (preliminary biphasic) segment(s).

Table S1. Heterogeneity test on sample wrRB – Preliminary to true digestogram phases.

Table S2. The digestion parameters and amylose contents of the white rice samples.

Table S3. The comparison of digestion parameters of the monophasic raw brown rice (rb) and raw white rice (wr).